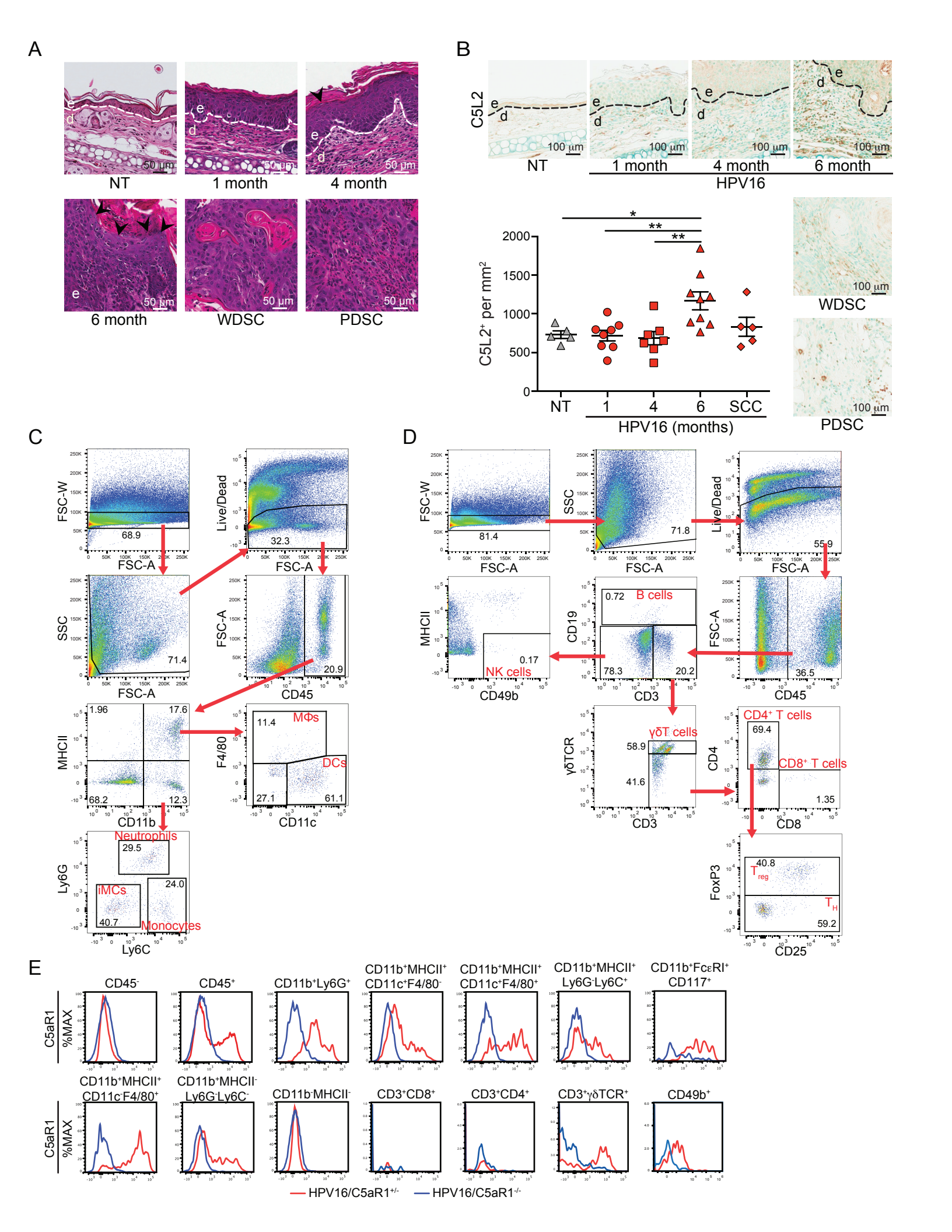
A
NT
1 month
4 month
6 month
WDSC
PDSC
50 μm
B
C5L2
100 μm
NT
1 month
4 month
6 month
HPV16
C5L2+ per mm2
2000
1500
1000
500
0
NT
1
4
6
SCC
HPV16 (months)
WDSC
PDSC
C
FSC-W
FSC-A
68.9
Live/Dead
32.3
SSC
71.4
CD45
20.9
MHCII
1.96
17.6
68.2
12.3
CD11b
F4/80
11.4
MΦs
DCs
27.1
61.1
CD11c
Neutrophils
29.5
Ly6G
iMCs
24.0
40.7
Monocytes
Ly6C
D
81.4
71.8
55.9
0.72
B cells
CD19
0.17
NK cells
CD49b
78.3
20.2
CD3
36.5
γδTCR
γδT cells
58.9
41.6
CD4+ T cells
69.4
CD4
CD8+ T cells
1.35
CD8
40.8
Treg
TH
59.2
FoxP3
CD25
E
CD45-
CD45+
CD11b+Ly6G+
CD11b+MHCII+ CD11c+F4/80-
CD11b+MHCII+ CD11c+F4/80+
CD11b+MHCII+ Ly6G-Ly6C+
CD11b+FcεRI+ CD117+
CD11b+MHCII+ CD11c-F4/80+
CD11b+MHCII- Ly6G-Ly6C-
CD11b-MHCII-
CD3+CD8+
CD3+CD4+
CD3+γδTCR+
CD49b+
C5aR1 %MAX
HPV16/C5aR1+/-
HPV16/C5aR1-/-

Figure S1, related to Figure 1

(A) Representative histology of ear or truncal skin from nontransgenic (NT) and HPV16 mice from indicated ages. Dotted line represents the dermal (d)-epidermal (e) junction and arrowheads depict areas of dysplasia.

(B) Immunodetection of C5L2 (brown staining, counterstained with methyl green; panels in top row and on side), and their quantification (bottom) from nontransgenic (NT) littermate ear skin, and canonical timepoints reflecting hyperplasia (1-month), early dysplasia (4-month), late dysplasia (6-month), well differentiated SCC (WDSC) and poorly differentiated SCC (PDSC) from HPV16 mice. Representative images are shown. Data points in graph reflect automated quantification (bottom left) of $C5L2^{+}$ infiltrating cells, with each data point reflecting an independent mouse. Significance determined by one-way ANOVA with Bonferroni post-test for multiple comparisons.

(C-D) Gating strategy for identification of myeloid (C) and lymphoid (D) lineages. Populations identified are depicted in red text.

(E) Flow cytometric analysis of C5aR1 expression on cells isolated from 4-month old HPV16/$C5aR1^{+/-}$ and HPV16/$C5aR1^{-/-}$ ears. Shown are representative histograms from 3-5 mice per group.

Data are represented as means ± SEM. * $p < 0.05$; ** $p < 0.01$; *** $p < 0.001$; **** $p < 0.0001$.

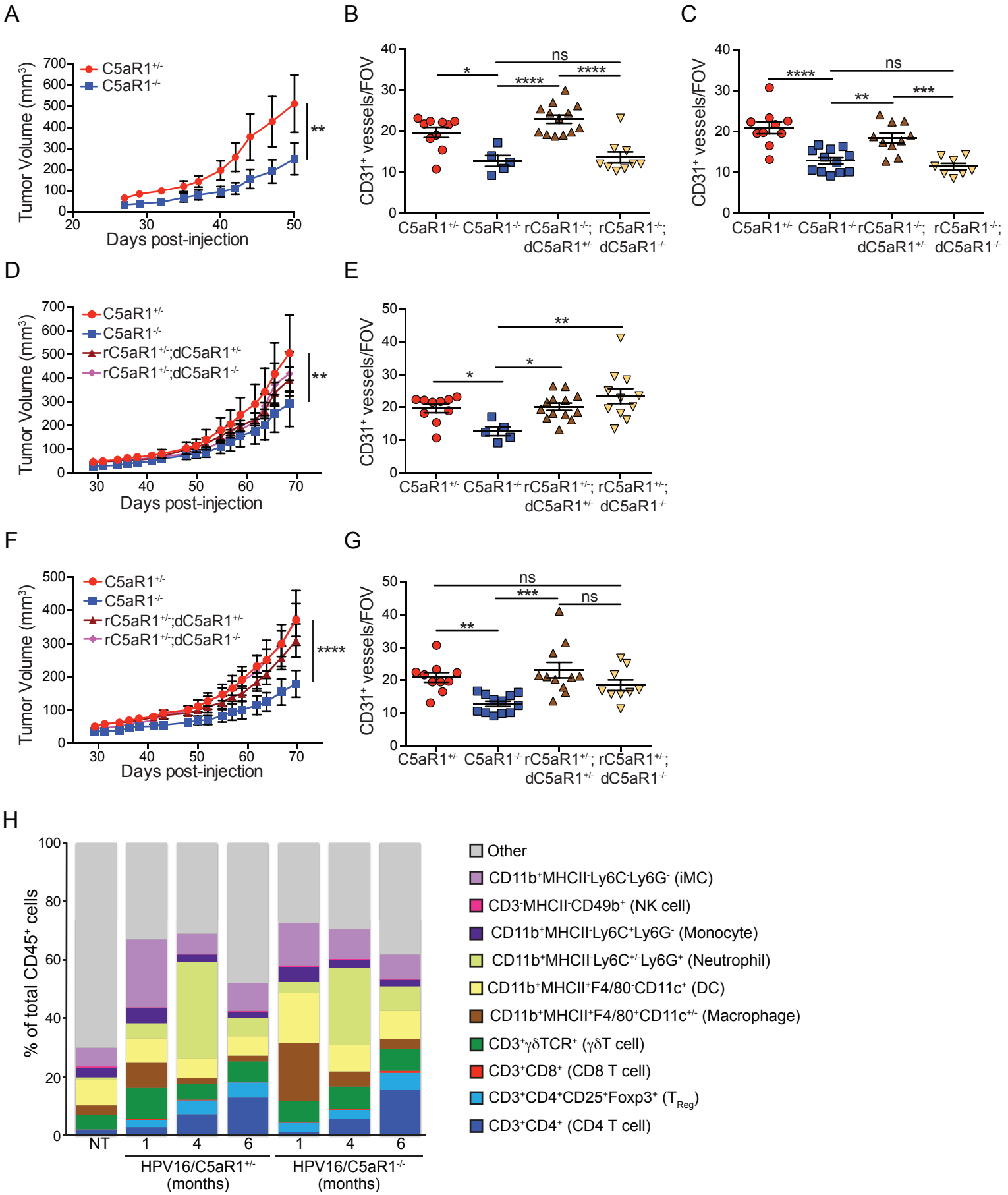
A
Tumor Volume (mm3)
Days post-injection
C5aR1+/-
C5aR1-/-
**
B
CD31+ vessels/FOV
ns
*
****
****
C5aR1+/-
C5aR1-/-
rC5aR1-/-; dC5aR1+/-
rC5aR1-/-; dC5aR1-/-
C
CD31+ vessels/FOV
****
ns
**
***
D
Tumor Volume (mm3)
Days post-injection
C5aR1+/-
C5aR1-/-
rC5aR1+/-;dC5aR1+/-
rC5aR1+/-;dC5aR1-/-
**
E
CD31+ vessels/FOV
**
*
*
F
Tumor Volume (mm3)
Days post-injection
C5aR1+/-
C5aR1-/-
rC5aR1+/-;dC5aR1+/-
rC5aR1+/-;dC5aR1-/-
****
G
CD31+ vessels/FOV
ns
***
ns
**
H
% of total CD45+ cells
NT
1
4
6
1
4
6
HPV16/C5aR1+/- (months)
HPV16/C5aR1-/- (months)
Other
CD11b+MHCII-Ly6C-Ly6G- (iMC)
CD3-MHCII-CD49b+ (NK cell)
CD11b+MHCII-Ly6C+Ly6G- (Monocyte)
CD11b+MHCII-Ly6C+/-Ly6G+ (Neutrophil)
CD11b+MHCII+F4/80-CD11c+ (DC)
CD11b+MHCII+F4/80+CD11c+/- (Macrophage)
CD3+γδTCR+ (γδT cell)
CD3+CD8+ (CD8 T cell)
CD3+CD4+CD25+Foxp3+ (TReg)
CD3+CD4+ (CD4 T cell)

Figure S2, related to Figure 1

(A) Growth curves of WDSC cells intradermally implanted into syngeneic C5aR1$^{+/-}$ and C5aR1$^{-/-}$ mice (n = 5-8 mice/group). Significance determined by two-way ANOVA with Bonferroni post-test for multiple comparisons.

(B) Quantitative analysis of tissue sections from end-stage SCCs (Figure 1G) for CD31^{+} vascular structures. Sections stained for CD31 and manual counting of CD31^{+} structures performed in 5 fields of view per SCC. Significance determined by one-way ANOVA with Bonferroni post-test for multiple comparisons. Each data point reflects quantitative data from an individual SCC.

(C) Quantitative analysis of tissue sections from end-stage SCCs from (Figure 1H) for CD31^{+} vascular structures. Sections stained for CD31 and manual counting of CD31^{+} structures performed in 5 fields of view per SCC. Significance determined by one-way ANOVA with Bonferroni post-test for multiple comparisons. Each data point reflects quantitative data from an individual SCC.

(D) C5aR1$^{+/-}$ or C5aR1$^{-/-}$ donor (d) BMMCs admixed 1:1 with PDSC5 cells and intradermally injected into syngeneic recipient (r) mice of indicated genotype. Mice from two independent experiments are depicted (n = 11-13 mice/group), with significance determined by two-way ANOVA and Bonferroni post-test for multiple comparisons.

(E) Quantitative analysis of tissue sections from end-stage SCCs from (Figure S2D) for CD31^{+} vascular structures. Sections stained for CD31 and manual counting of CD31^{+} structures performed in 5 fields of view/SCC. Significance determined by one-way ANOVA with Bonferroni post-test for multiple comparisons. Each data point reflects quantitative data from an individual SCC.

(F) C5aR1$^{+/-}$ or C5aR1$^{-/-}$ donor (d) BMMΦs admixed 1:1 with PDSC5 cells and intradermally injected into syngeneic recipient (r) mice of indicated genotype. Mice from two independent experiments depicted (n = 12-15 mice/group), with significance determined by two-way ANOVA and Bonferroni post-test for multiple comparisons.

(G) Quantitative analysis of tissue sections from end-stage tumors from (Figure S2F) for CD31^{+} vascular structures. Sections stained for CD31 and manual counting of CD31^{+} structures performed in 5 fields of view/SCC. Significance determined by one-way ANOVA with Bonferroni post-test for multiple comparisons. Each data point reflects quantitative data from an individual SCC.

(H) Immune complexity of ear skin from HPV16 mice of the indicated genotypes at indicated timepoints. Results are shown as percentage of total live CD45^{+} cells, with significance determined by Student's t test. N=4-5 mice/group. Colors reflect distinct cell lineages as determined by lineage-selective expression of epitopes shown. Gating strategy shown in Figure S1C-D.

Data are represented as means ± SEM. * $p < 0.05$; ** $p < 0.01$; *** $p < 0.001$; **** $p < 0.0001$.

A

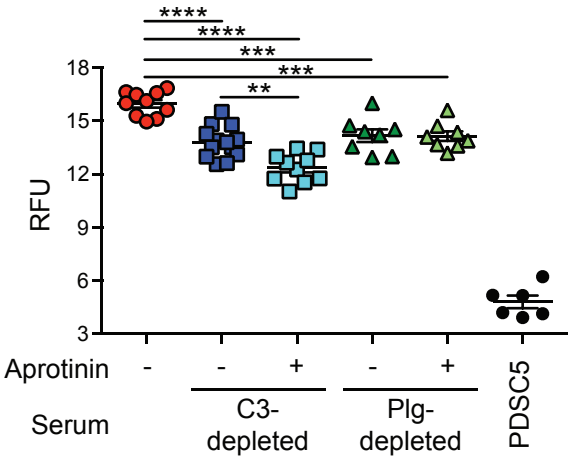
****
****
***
***
**
18
15
12
9
6
3
RFU
Aprotinin
-
-
+
-
+
Serum
C3-depleted
Plg-depleted
PDSC5

B

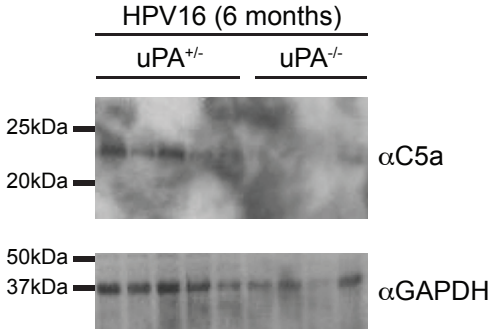
HPV16 (6 months)
uPA+/-
uPA-/-
25kDa
20kDa
αC5a
50kDa
37kDa
αGAPDH

Figure S3, related to Figure 3

(A) In vitro complement deposition assay of BMMΦs derived from nontransgenic mice co-cultured with PDSC5 cells in the presence of indicated serum +/- aprotinin, and IF-stained for C5a and F4/80. Quantitation of IF staining for C5a deposition determined by ImageJ from one independent regions of interest (ROIs) per tissue culture well with each experimental condition replicated in 8-12 wells, for each experimental condition indicated and the experiment repeated once. Data points shown reflect mean ± SEM.

(B) Immunoblot of C5a (top) and GAPDH (bottom) lysates from ear skin of 6-month old HPV16 mice of indicated genotype. Blots shown were cropped at the edges.

A

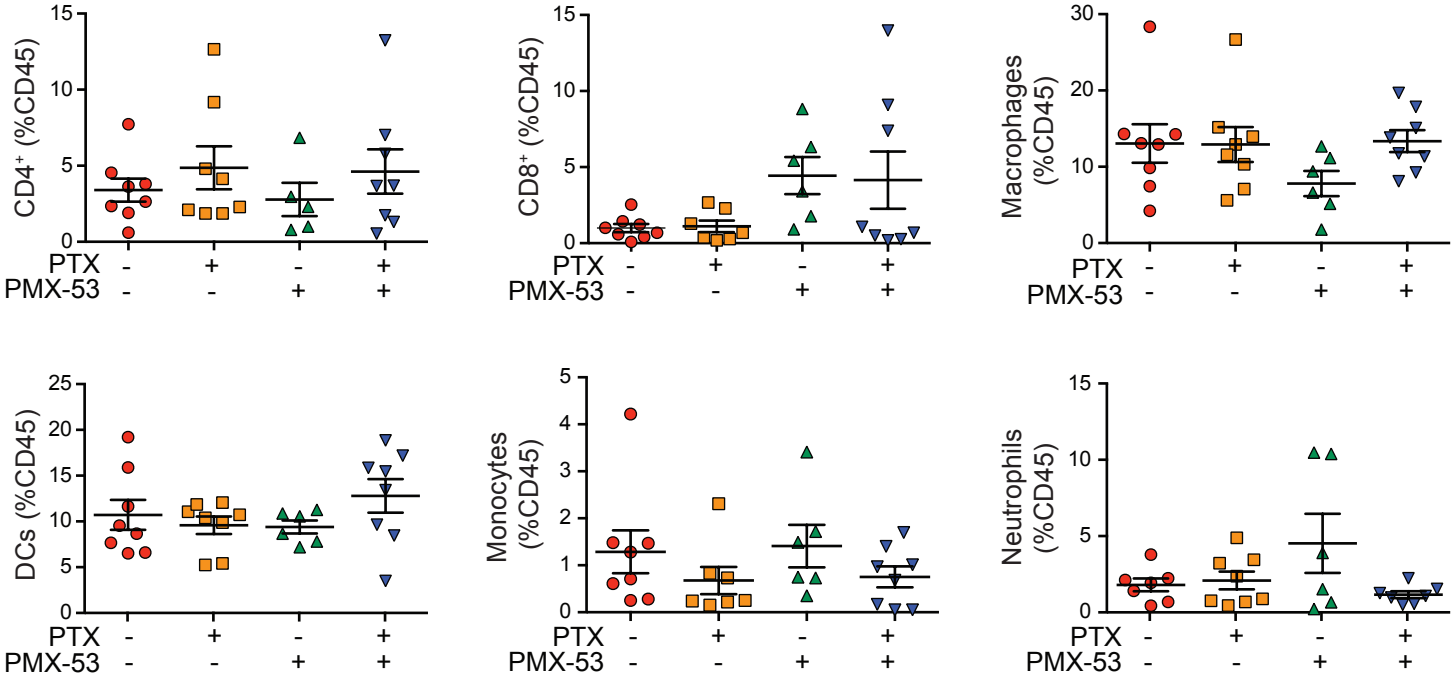
CD4⁺ (%CD45)
CD8⁺ (%CD45)
Macrophages (%CD45)
DCs (%CD45)
Monocytes (%CD45)
Neutrophils (%CD45)
PTX
PMX-53

B

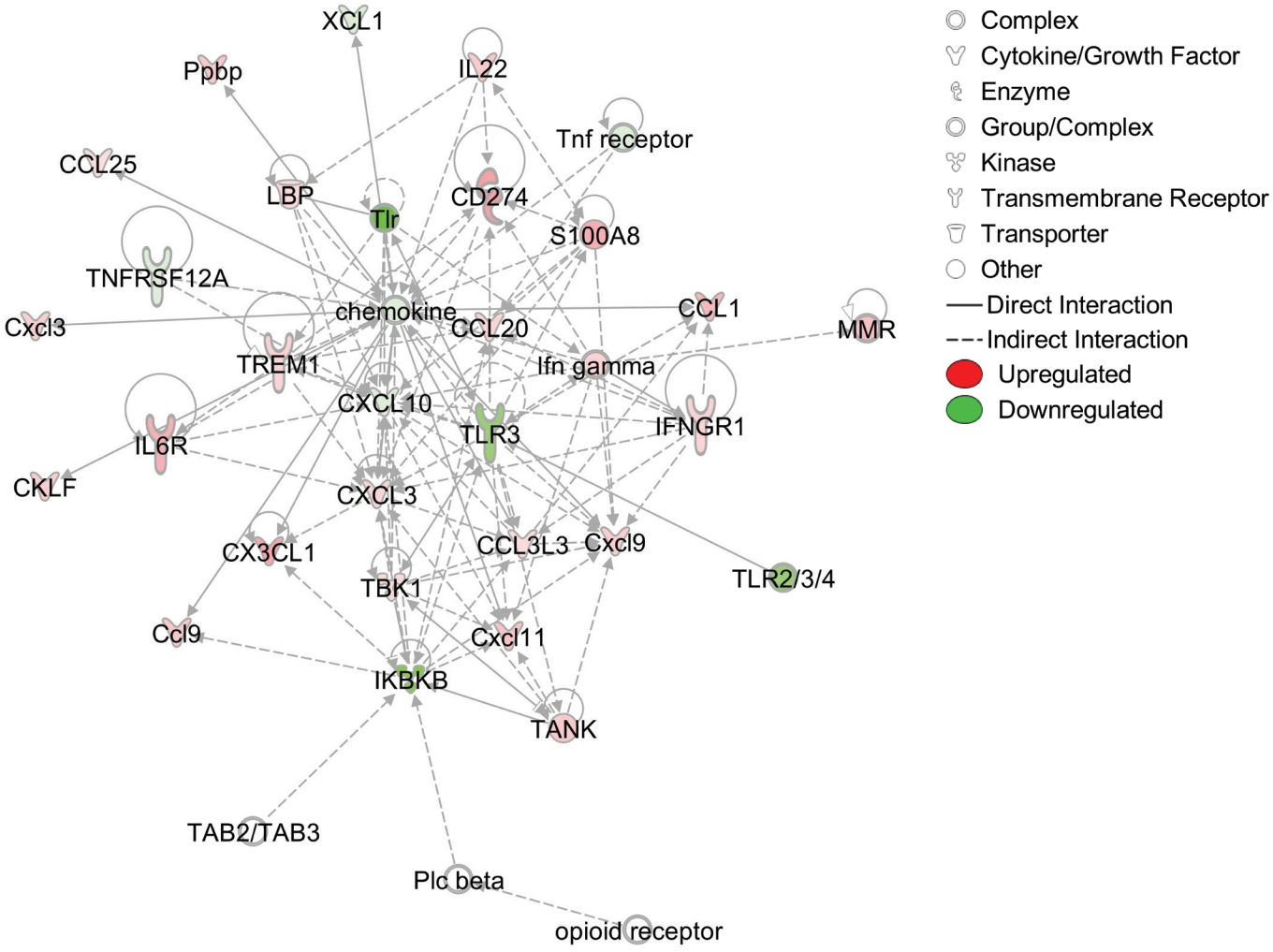
XCL1
Ppbp
IL22
Tnf receptor
CCL25
LBP
Tlr
CD274
S100A8
TNFRSF12A
Cxcl3
chemokine
CCL20
CCL1
MMR
TREM1
Ifn gamma
CXCL10
TLR3
IFNGR1
IL6R
CKLF
CXCL3
CX3CL1
CCL3L3
Cxcl9
TLR2/3/4
TBK1
Ccl9
Cxcl11
IKBKB
TANK
TAB2/TAB3
Plc beta
opioid receptor
Complex
Cytokine/Growth Factor
Enzyme
Group/Complex
Kinase
Transmembrane Receptor
Transporter
Other
Direct Interaction
Indirect Interaction
Upregulated
Downregulated

Figure S4, related to Figure 6

(A) Flow cytometric analysis of SCCs isolated at end stage from mice in Figure 6B for $CD4^+$ T cells ($CD3^+CD4^+$), $CD8^+$ T cells ($CD3^+CD8^+$), Macrophages ($CD11b^+MHCII^+F4/80^+CD11c^{+/-}$), DCs ($CD11b^+MHCII^+F4/80^-CD11c^+$), monocytes ($CD11b^+MHCII^-Ly6C^+Ly6G^-$), and neutrophils ($CD11b^+MHCII^-Ly6C^{+/-}Ly6G^+$), as percentages of live $CD45^+$ cells, with significance determined by one-way ANOVA and Bonferroni post-test for multiple comparisons. Each data point reflects quantitative data from an individual SCC.

(B) IPA network analysis of gene expression from $CD11b^+MHCII^+F4/80^+CD11c^{+/-}$ macrophages isolated from SCCs of PMX-53/PTX treated mice, as compared to PMX-53 monotherapy. Chosen network consists of the top scoring network containing a molecule (score = 33) from Figure 6E (interferon γ). Color intensity of shapes is directly related to the level of upregulation (red) or downregulation (green).

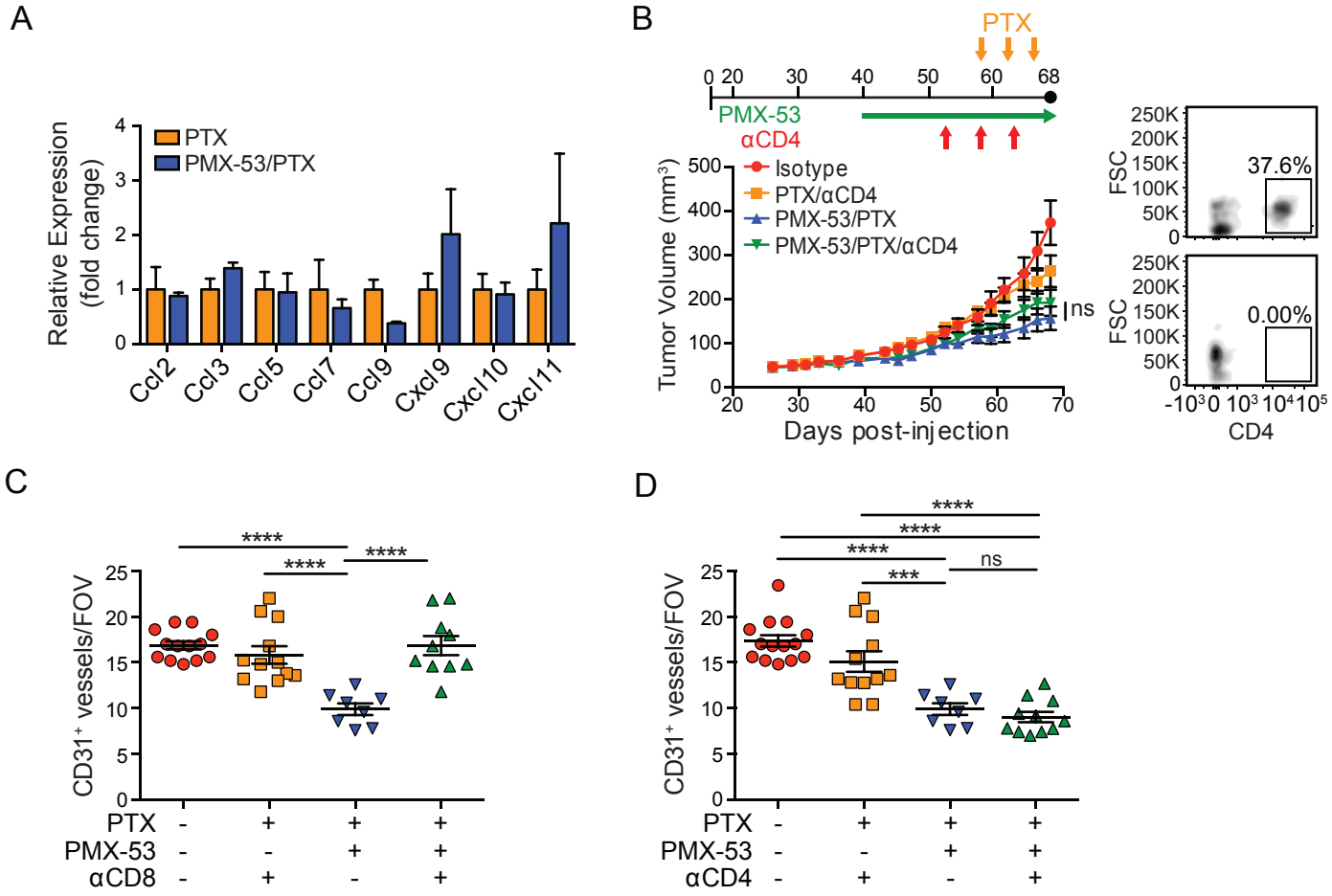
A
Relative Expression (fold change)
PTX
PMX-53/PTX
Ccl2
Ccl3
Ccl5
Ccl7
Ccl9
Cxcl9
Cxcl10
Cxcl11
B
PTX
PMX-53
αCD4
Isotype
PTX/αCD4
PMX-53/PTX
PMX-53/PTX/αCD4
Tumor Volume (mm³)
Days post-injection
ns
FSC
CD4
37.6%
0.00%
C
CD31⁺ vessels/FOV
PTX
PMX-53
αCD8
D
CD31⁺ vessels/FOV
PTX
PMX-53
αCD4
ns

Figure S5, related to Figure 6

(A) Chemokine mRNA expression in FACS-sorted $CD11b^{+}MHCII^{+}F4/80^{+}$ macrophages from end-stage tumors (Figure 6B) as determined by qPCR. Depicted are relative mRNA levels normalized to *Tbp* in macrophages from 4 mice/treatment group.

(B) Dosing strategies (top) for evaluating tumor growth kinetics (lower graph) of PDSC5-SCCs in syngeneic mice treated with PTX or PMX-53/PTX, and either isotype control (IgG2b) or αCD4 mAb. Shown are mice pooled from 2 independent experiments (n=8-11 mice/group). Significance determined by two-way ANOVA with Bonferroni post-test for multiple comparisons. At right is FACS plot showing percentage $CD4^{+}$ cells in SCCs from control (top) versus CD4-depleted (bottom) mice.

(C-D) Quantitation of $CD31^{+}$ vessels in tissue sections from end-stage SCCs shown in Figure 6F (C) and Figure S4B (D). CD31 positivity was analyzed manually in 5 fields of view/end-stage SCC, with significance determined by one-way ANOVA and Bonferroni post-test for multiple comparisons.

Data are represented as means ± SEM. * $p < 0.05$; ** $p < 0.01$; *** $p < 0.001$; **** $p < 0.0001$.

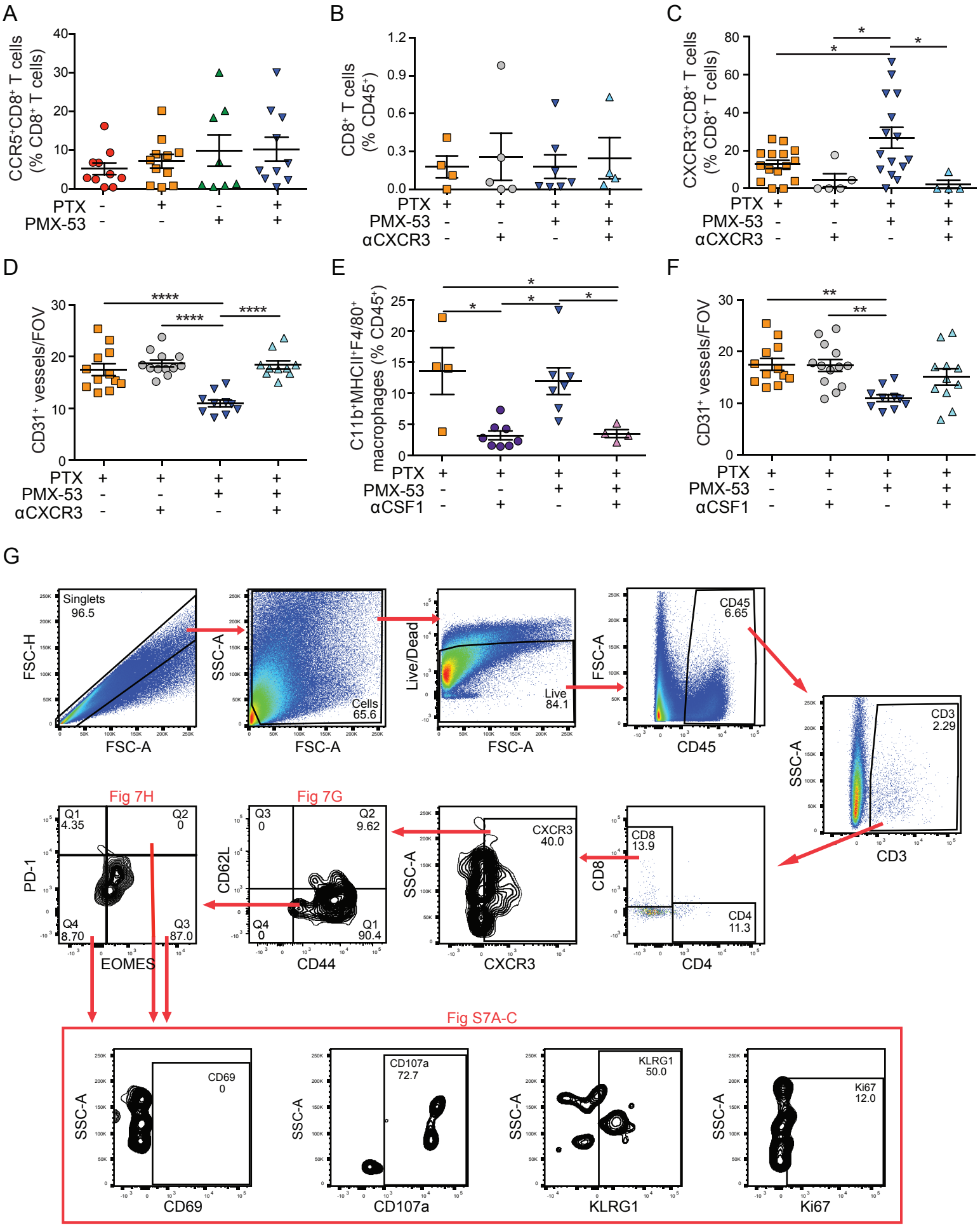
A
CCR5+CD8+ T cells (% CD8+ T cells)
PTX
PMX-53
B
CD8+ T cells (% CD45+)
PTX
PMX-53
αCXCR3
C
CXCR3+CD8+ T cells (% CD8+ T cells)
PTX
PMX-53
αCXCR3
D
CD31+ vessels/FOV
PTX
PMX-53
αCXCR3
E
C11b+MHCII+F4/80+ macrophages (% CD45+)
PTX
PMX-53
αCSF1
F
CD31+ vessels/FOV
PTX
PMX-53
αCSF1
G
Singlets 96.5
FSC-H
FSC-A
SSC-A
Cells 65.6
Live/Dead
Live 84.1
CD45 6.65
CD45
CD3 2.29
CD3
Fig 7H
Q1 4.35
Q2 0
Q4 8.70
Q3 87.0
PD-1
EOMES
Fig 7G
Q3 0
Q2 9.62
Q4 0
Q1 90.4
CD62L
CD44
CXCR3 40.0
CXCR3
CD8 13.9
CD4 11.3
CD8
CD4
Fig S7A-C
CD69 0
CD69
CD107a 72.7
CD107a
KLRG1 50.0
KLRG1
Ki67 12.0
Ki67

Figure S6, related to Figure 7

(A) Flow cytometric analysis assessing infiltration of $CCR5^+$ $CD8^+$ T cell into SCCs from mice treated as in Figure 6B, with significant differences determined by one-way ANOVA and Bonferroni post-test for multiple comparisons.

(B) Flow cytometric analysis assessing infiltration of total $CD8^+$ T cells in SCCs of mice treated with αCXCR3 mAb. Significance determined by one-way ANOVA with Bonferroni post-test for multiple comparisons.

(C) Flow cytometric analysis of SCCs in mice treated with αCXCR3 mAb. Significance determined by one-way ANOVA with Bonferroni post-test for multiple comparisons.

(D) Quantitation of $CD31^+$ vessels in tissue sections from end-stage SCCs (Figure 7C). Sections stained for CD31 and manual counting of $CD31^+$ structures performed in 5 fields of view/SCC. Significance determined by one-way ANOVA with Bonferroni post-test for multiple comparisons.

(E) Flow cytometric analysis of $CD11b^+MHCII^+F4/80^+$ macrophage presence in SCCs isolated from mice from Figure 7D. Significance determined by one-way ANOVA with Bonferroni post-test for multiple comparisons.

(F) Quantitation of $CD31^+$ vessels in tissue sections from end-stage SCCs end-stage SCCs isolated from mice from Figure 7D. Sections stained for CD31 and manual counting of $CD31^+$ structures performed in 5 fields of view/mouse. Significance determined by one-way ANOVA with Bonferroni post-test for multiple comparisons.

(G) Gating strategy for determining immune populations depicted in Figures 7G-H and S7A-C.

In panels A-F, each data point reflects quantitative data from an individual SCC. Data are represented as means $\pm$ SEM. * $p < 0.05$; ** $p < 0.01$; *** $p < 0.001$; **** $p < 0.0001$.

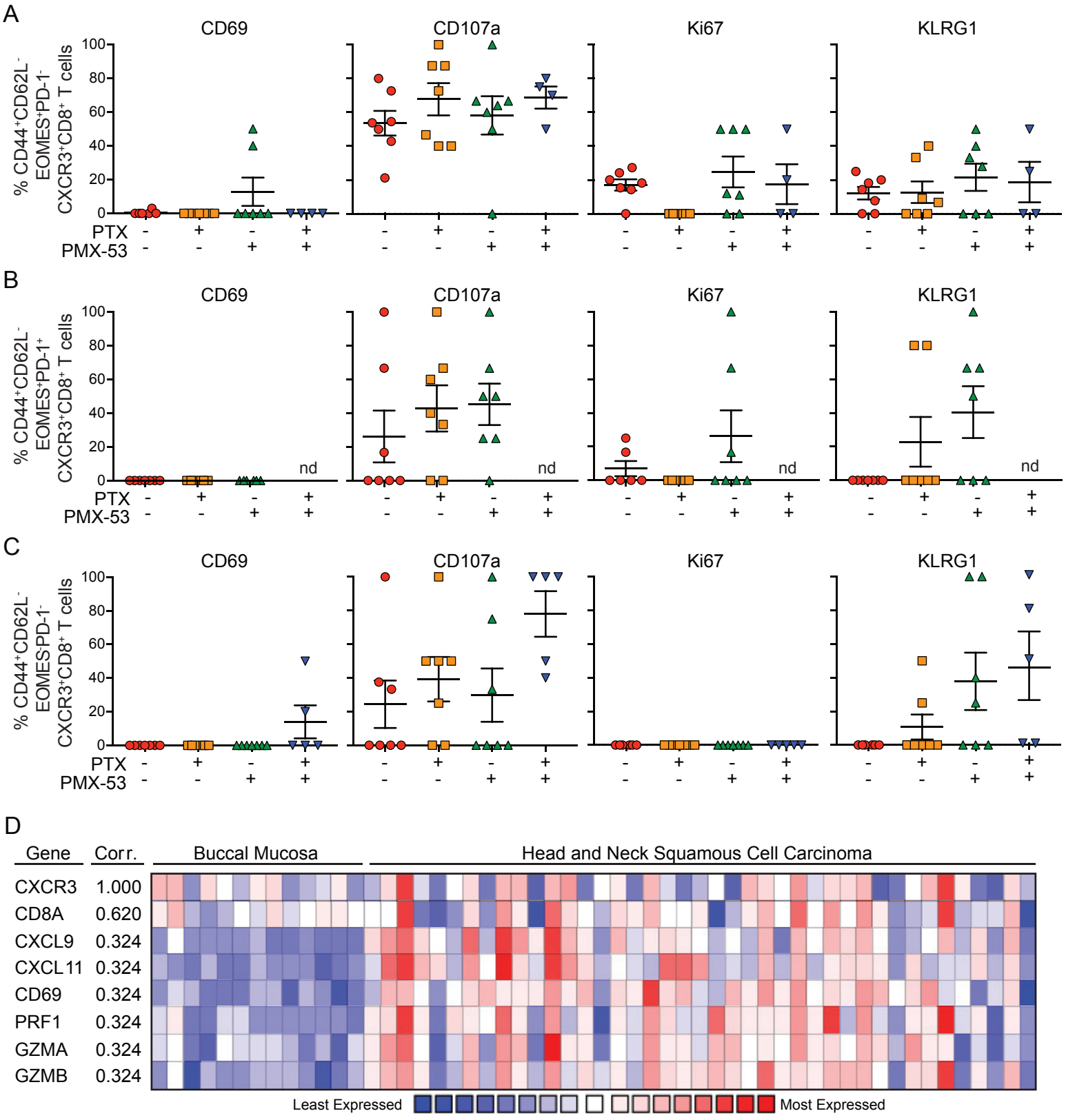
A
CD69
CD107a
Ki67
KLRG1
% CD44+CD62L- EOMES+PD-1- CXCR3+CD8+ T cells
100
80
60
40
20
0
PTX - + - +
PMX-53 - - + +
B
CD69
CD107a
Ki67
KLRG1
% CD44+CD62L- EOMES+PD-1+ CXCR3+CD8+ T cells
nd
PTX - + - +
PMX-53 - - + +
C
CD69
CD107a
Ki67
KLRG1
% CD44+CD62L- EOMES-PD-1- CXCR3+CD8+ T cells
PTX - + - +
PMX-53 - - + +
D
Gene
Corr.
Buccal Mucosa
Head and Neck Squamous Cell Carcinoma
CXCR3 1.000
CD8A 0.620
CXCL9 0.324
CXCL11 0.324
CD69 0.324
PRF1 0.324
GZMA 0.324
GZMB 0.324
Least Expressed
Most Expressed

Figure S7, related to Figure 7

(A-C) Flow cytometric analysis of CD69, CD107a, Ki67, and KLRG1 on $CD44^+CD62L^-EOMES^+PD\text{-}1^-$ (A) $CD44^+CD62L^-EOMES^+PD\text{-}1^+$ (B), and $CD44^+CD62L^-EOMES^-PD\text{-}1^-$ (C) $CXCR3^+CD8^+$ T cells. Significance determined by one-way ANOVA with Bonferroni post-test for multiple comparisons. 'nd' indicates that the parent population was not detected.

(D) Correlation (Corr.) between *CXCR3* and *CD8A*, *CXCL9*, *CXCL11*, *CD69*, *PRF1*, *GZMA*, and *GZMB* in the Ginos Head-Neck dataset using Oncomine coexpression heatmaps. Correlation derived from the average linkage hierarchical clustering and data displayed as log2 median-centered intensity with lowest expression in blue and highest expression in red.

In panels A-C, each data point reflects quantitative data from an individual SCC. Data represented as means ± SEM. * $p < 0.05$; ** $p < 0.01$; *** $p < 0.001$; **** $p < 0.0001$.

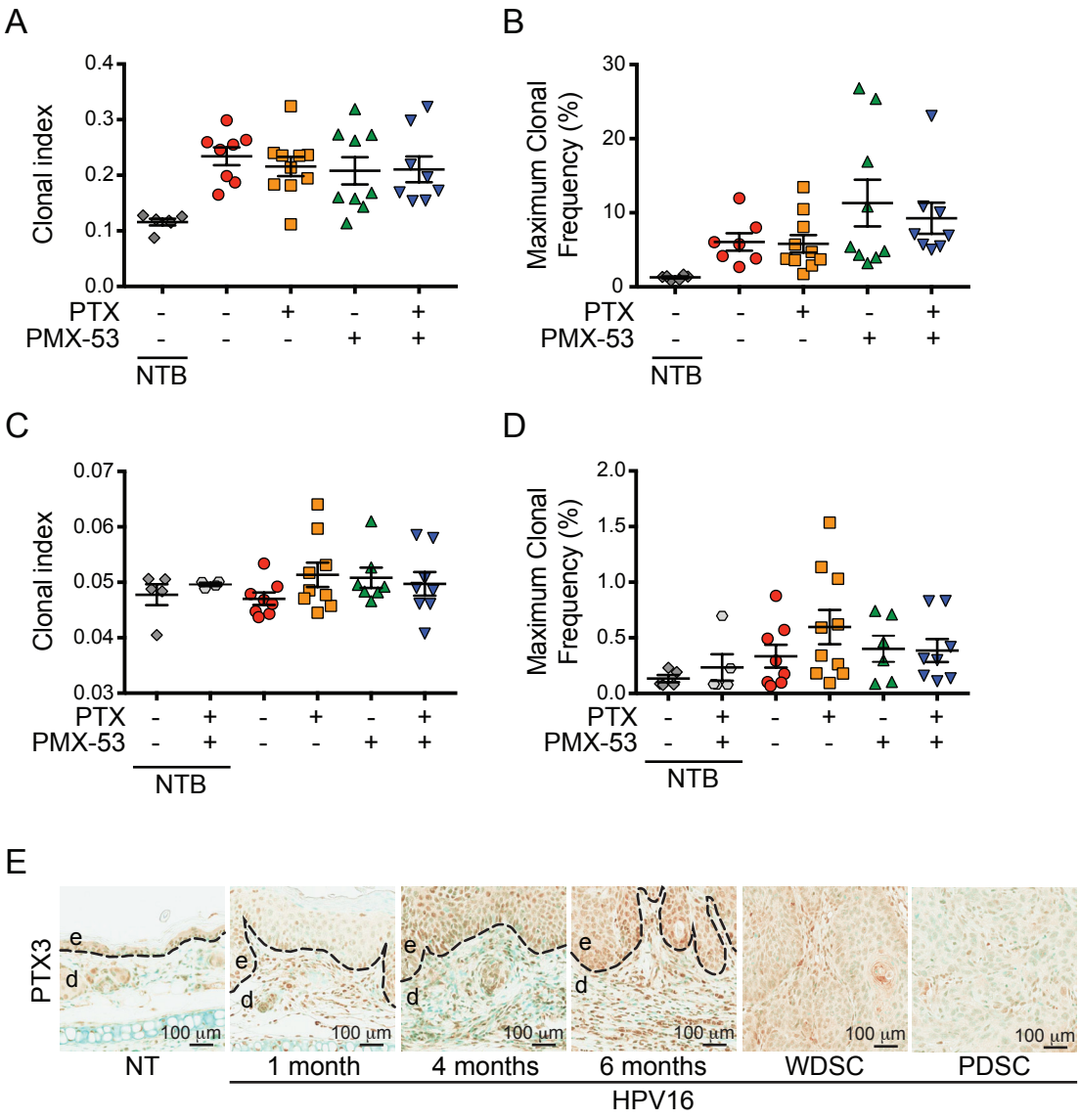
A
Clonal index
0.4
0.3
0.2
0.1
0.0
PTX - - + - +
PMX-53 - - - + +
NTB
B
Maximum Clonal Frequency (%)
30
20
10
0
PTX - - + - +
PMX-53 - - - + +
NTB
C
Clonal index
0.07
0.06
0.05
0.04
0.03
PTX - + - + - +
PMX-53 - + - - + +
NTB
D
Maximum Clonal Frequency (%)
2.0
1.5
1.0
0.5
0.0
PTX - + - + - +
PMX-53 - + - - + +
NTB
E
PTX3
e
d
100 µm
NT
1 month
4 months
6 months
WDSC
PDSC
HPV16

Figure S8, related to Figure 8

(A-D) Matched end-stage SCCs and PBMCs from mice of specified treatment groups vs. nontumor bearing (NTB) mice analyzed by deep sequencing of the CDR3 region of the TCRβ chain.

(A and C) Clonal index of SCCs (A) and PBMCs (C).

(B and D) Clonal frequency of most frequent TCR clonotype in SCCs (B) and PBMCs (D).

Each data point in A-D reflects quantitative data from an individual SCC or nontumor-bearing mouse.

(E) Immunodetection of PTX3 (brown staining, counterstained with methyl green; panels in top row and on side), and quantification (bottom) from nontransgenic (NT) littermate ear skin, and canonical timepoints reflecting hyperplasia (1-month), early dysplasia (4-month), late dysplasia (6-month), well differentiated SCC (WDSC) and poorly differentiated SCC (PDSC) from HPV16 mice. Representative images are shown.